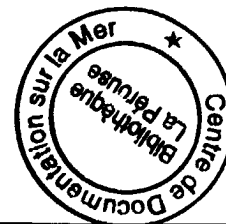


# Phosphorites from the Oman Margin, ODP Leg 117

Phosphorites  
Oman margin  
ODP Leg 117  
Phosphatization  
Apatite

Phosphorites  
Marge d'Oman  
Leg ODP 117  
Phosphatisation  
Apatite



Venigalla PURNACHANDRA RAO <sup>a</sup> and Michel LAMBOY <sup>b</sup>

<sup>a</sup> National Institute of Oceanography, Dona Paula , 403 004, Goa, India.

<sup>b</sup> Department of Geology, University of Rouen, 76821 Mont-Saint-Aignan Cedex, France.

Received 23/05/94, in revised form 24/11/94, accepted 27/11/94.

## ABSTRACT

The phosphorite levels present in the ODP cores of the Oman margin are of two types: (a) sediment levels dominated by phosphate grains with a few white to light-brown nodules; these are sandy and predominantly occur in Upper Miocene to Early Pliocene sediments; and (b) sediment levels poor in phosphatic grains but consisting of several brown to dark-brown nodules; these mainly occur in Late Pliocene to Early Pleistocene sediments wherein some levels are sandy while others are clayey. The phosphate grains occur as coprolites, faecal pellets, spherical and coated grains, micronodules, foraminifer infillings and bone fragments.

Ovoid to rod-shaped and botryoid-type apatite microparticles resembling phosphatized bacteria or coalesced bacteria are common in porous areas of all types of phosphate grains and nodules. Phosphatized extracellular remnants such as polyhedral cell units and spherical cavities are also present. The compact structures seem to consist of tightly packed ovoids or botryoids and/or to be formed by the overgrowth of phosphate. The initial morphology of the grains/nodules was largely preserved; the light-coloured dull grains are more porous, heterogeneous and appear less evolved, whereas dark brown shiny grains are mostly compact, tend to be homogeneous and appear highly evolved. It appears that phosphatization took place within the initial supports and was controlled by microenvironments, duration and source metals.

The sediment levels dominated by phosphate grains are bioturbated and associated with shallow water oxic conditions and lowest sedimentation rates. Bioturbation probably favoured the production of different initial substrates which subsequently phosphatized. Light-brown nodules are formed by a rapid, early diagenetic process. The abundant nodule formation in the Late Pliocene - Early Pleistocene sediments is favoured by the deepening of the Oman margin which took place during the Late Pliocene and the establishment of an oxygen minimum zone at about this time. Unlike the Peru margin phosphorites, the Oman margin phosphorites lack conglomeratic nodules, phosphorite crusts formed in hardgrounds and thick phosphatic sandy beds and glauconites. Fe-recycling is not important in the formation of Oman margin phosphorites. The reworked nature of organic matter, the less pronounced oxygen minimum zone and high sedimentation rates are probably responsible for the apparent absence of present day phosphorites on the Oman margin.

## RÉSUMÉ

## Les phosphorites de la marge d'Oman, Leg ODP 117.

Les niveaux phosphatés présents dans les forages ODP de la marge d'Oman sont de deux types : a) lits de sédiments dominés par des grains de phosphate avec quelques nodules blanc à brun clair ; ils sont sableux et cantonnés surtout du Miocène supérieur au Pliocène basal. b) Lits de sédiments pauvres en grains de phosphate mais contenant des nodules brun à brun foncé ; quelques-uns de ces lits sont sableux, les autres argileux ; ils se trouvent surtout du Pliocène terminal au début du Pleistocène. Les grains de phosphate sont des coprolites, des pelotes fécales, des grains sphériques, des grains enrobés, des micronodules, des remplissages de foraminifères et des fragments d'os.

Les microparticules d'apatite en forme d'ovoïde ou de bâtonnet et celles de type botryoidal, ressemblant à des bactéries ou des colonies bactériennes phosphatées, sont communément présentes dans les zones poreuses de tous les types de phosphate en nodules et en grains. Les structures compactes semblent être des ovoïdes ou des botryoïdes comprimés et/ou se sont formées par surcroissance du phosphate. La morphologie des grains et des nodules a été souvent conservée ; la couleur d'une macroparticule et son aspect interne poreux/compact peuvent être reliés au degré d'évolution du phosphate à l'intérieur de la particule. Les grains clairs et ternes, plus poreux et hétérogènes, paraissent peu évolués alors que les grains foncés et brillants sont surtout compacts, tendent vers l'homogénéité et paraissent fortement évolués. Il apparaît que la phosphatation prit place au sein de supports initiaux et fut contrôlée par les microenvironnements, la durée et probablement la source des éléments.

Les niveaux sédimentaires où les grains de phosphate dominent sont bioturbés et associés à des conditions d'eaux peu profondes et oxygénées ainsi qu'aux plus faibles taux de sédimentation. La bioturbation a probablement favorisé la production de certains supports initiaux phosphatisés par la suite. Les nodules se sont formés par des processus de diagenèse précoce rapides. L'enfoncement de la marge d'Oman survint à la fin du Pliocène et la zone d'oxygène minimum s'établit à peu près à ce moment ; ceci favorisa probablement la formation de nodules dans les sédiments durant la fin du Pliocène et le début du Pleistocène. Contrairement aux phosphorites de la marge du Pérou, celles de la marge d'Oman manquent de nodules conglomératiques, de croûtes phosphatées associées à des hardgrounds ainsi que d'épais niveaux de sables phosphatés et de glauconie. Le processus de recyclage par le fer ne semble pas important dans la formation des phosphorites de la marge d'Oman. La nature remaniée de la matière organique, une zone d'oxygène minimum moins prononcée et de forts taux de sédimentation sont probablement responsables de l'absence apparente de phosphatogenèse actuelle sur la marge d'Oman.

*Oceanologica Acta*, 1995, 18, 3, 289-307

## INTRODUCTION

Phosphorites are found in practically all geological ages starting from the Precambrian. It appears, however, that certain periods are more favourable for phosphorite formation than others. Several mechanisms explain the distribution of phosphorites through time. The consensus is that there is no single mechanism to explain all the phosphorites (Cook and McElhinny, 1979; Parrish, 1990), and that each deposit is governed by a combination of several favourable conditions. On the other hand, most of the ancient phosphorites are pelletal and larger in areal extent; some are associated with glaucony facies. Modern phosphorites are mostly crusts and nodules with few pellets and are sparsely distributed on the sea floor. In view of this, Bentor (1980) thought that the Recent phosphorites are poor analogues for their ancient counterparts. Glenn *et al.*

(1994), however, showed that the Modern Peru margin phosphorites are much more larger than previously assumed and are comparable with the size of many ancient phosphorites. The main purpose of this paper is to investigate the petrology, mineralogy, and geochemistry of phosphorites (Miocene to Pleistocene) recovered from ODP (Ocean Drilling Program) Leg 117, off the Oman margin, northwest Arabian Sea, in order to understand their origin.

The Oman continental margin and the Peru margin have both similarities and dissimilarities in their settings. Upwelling occurs and the mean accumulation rates of organic carbon are similar on both margins (Emeis *et al.*, 1991). Modern phosphorites occur on the Peru margin but not on the Oman margin. We compare the results reported here with the phosphorites recovered during ODP Leg 112 from the Peru margin (Suess *et al.*, 1988; Garrison and Kastner, 1990; Lamboy, 1994) and assess the controlling factors on phosphorite formation.

## MATERIALS AND METHODS

ODP Leg 117 investigated the continental slope off Oman and the Owen ridge, northwest Arabian Sea (Fig. 1) (Prell *et al.*, 1989). Phosphorite nodules and phosphatic sediments were recovered only in the cores of sites located on the upper continental slope. Based on the observations reported in the Initial Reports of ODP Leg 117, samples were selected and sampled by one of us from several phosphatic levels (Tab. 1) in three cores stored at the Gulf Coast Repository, College Station, Texas. Most of the phosphatic levels studied here correspond to the cores of site 726 (Tab. 1, Fig. 2).

Polished and thin sections were made for phosphorite nodules and phosphatic grains. Freshly broken surfaces of some 350 fragments of nodules and grains were examined under the scanning electron microscope (SEM). Mineralogy was determined by X-ray diffraction. The sample powders were scanned from 8 to 60° 2 $\theta$  at 1° 2 $\theta$  / min. on a Philips X-ray diffractometer (PW 1840 model), using nickel filtered Cu K $\alpha$  radiation. Following Gulbrandsen (1970), the structural CO<sub>2</sub> content of CFA was estimated using (004) and (410) diffraction peaks and "a" cell dimensions of CFA were also calculated. Microanalysis of major elements was carried out by SEM-tied-EDS for different apatite microparticles, adjacent compact structures and other associated detrital and authigenic components in nodules and in grains. A total of 78 analyses were made.

## PREVIOUS WORK AND PHYSIOGRAPHIC SETTING

Phosphorite studies in the Indian Ocean date back to 1872, when *HMS Challenger* collected the first phosphorite samples from the ocean floor on the Agulhas Bank off Southeast Africa (Murray and Renard, 1891). These are

Oligocene to Miocene in age, and occur at a water depth of 100-500 m. The other phosphorites reported near the ODP Leg 117 are Error seamount phosphorites of Lower Oligocene to Miocene and Quaternary age (Rao *et al.*, 1992) and Socotra Island phosphorites of Meso- to Cenozoic age (Gevork'yon and Chugunyy, 1970). Phosphatized limestones and phosphate-glaucyony sediments of Late Quaternary age (Baturin, 1982; Rao *et al.*, 1990, 1993) were also reported from the western continental margin of India.

The Oman continental margin (Fig. 1) is characterized by a narrow continental shelf (25 km) over much of the region but wider (75 km) in certain places (Prell *et al.*, 1989). The continental slope is characterized by a series of linear north- to northeast-trending sediment terraces underlain by sedimentary basins. Seismic profiles show that the sediments in these basins are structurally isolated by faults with the exception of the shallowest few hundred metres (Mountain and Prell, 1989). Site 726, where maximum phosphate levels are found, is located on the continental shelf at 330 m water depth. The sediments recovered at this site may be divided into two units (Fig. 2) (Prell *et al.*, 1989). Unit II sediments are the oldest (Eocene I) and consist of shallow-water algal-foraminiferal and dolomitic limestones showing vadose diagenetic cements. Unit II sediments are unconformably overlain by Unit I sediments ranging from Miocene to Holocene. The Miocene - Pliocene sediments of this section were accumulated at 15 m/my and consist of a suite of laminated organic-rich silty clays interbedded with coarse grained phosphatic lag deposits (Prell *et al.*, 1989). The Pleistocene to Holocene sediments are calcareous silty clays and accumulated at about 45 m/my. The Holocene accumulation rates of the slope sediments at other sites of the continental margin range between 80 and 150 m/my. Several sediment intervals on this margin are bioturbated, even though oxygen values in the bottom waters are as low as 0.2 ml/l.

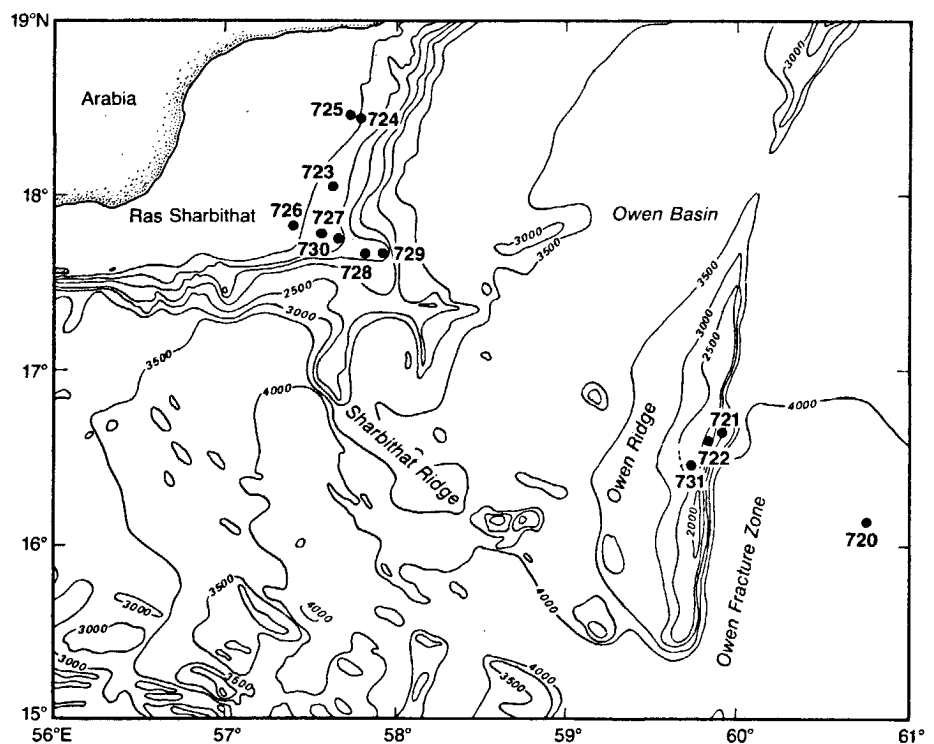


Figure 1

Location of ODP Leg 117 sites, NW Arabian Sea (from Prell *et al.*, 1989).

Table 1

*Details of the sediments and nodules studied from Leg 117.*

N° of samples	Type of sediment	Nodules	Dominant components in the sediment coarse fraction	Age
1. 724A 5H 6 69-71 cm	calcareous silty clay	brown (2 cm)	—————	Pleistocene
2. 724B 5H 2 142-143 cm	calc. silty clay	brown (0.5 cm)	—————	Pleistocene
3. 724B 5H 2 146-147 cm	calc. silty clay	light brown (0.5 cm)	—————	Pleistocene
4. 724B 18X 5 116-117 cm	clay	—————	bone fragments	Upper Pliocene
5. 724B 18X 5 124-125 cm	clay	—————	bone fr. & few phosphate grains	Upper Pliocene
6. 725C 11X 1 134-135 cm	clay	white(copronodule)	mostly unphosphatized planktonics, few quartz & bone fr.	Pleistocene
7. 726A 2H 6 78-79 cm	sand	dark brown(0.8cm)	mostly unphosphatized planktonics, few pellets & micronod.	Pleistocene
8. 726A 2H 6 80-81 cm	clayey silt	brown (0.5 cm)	—————	Pleistocene
9. 726A 3H 3 40-41 cm	sand	dark brown	mostly unphosphatized planktonics, (1.0 cm) few micronodules, coated grains, pellets & bone fr.	Pleistocene
10. 726A 3H 7 20-21 cm	clayey sand	—————	mostly unphosphatized planktonics, few bone fr. and micronodules	Pleistocene
11. 726A 6H 6 12-14 cm	sandy clay	dark brown (0.5 cm)	phos. sand with micronodules, coprolites, pellets, few bone fr. & planktonics	Pleistocene
12. 726A 6H 6 66-68 cm	silty clay	dark brown (1.5 cm)	—————	Pleistocene
13. 726A 6H 6 104-106 cm	sand	—————	unphosphatized planktonics, bone fr., micronod. & pellets	Pleistocene
14. 726A 7X 1 53-55 cm	clay	dark brown (0.5 cm)	mostly unphosphatized planktonics, gypsum , few phosphate grains	Pleistocene
15. 726A 7X 6 26-28 cm	sand	dark brown (1.0 cm)	phosphatic sand with micronodules, pellets, bone fr. & coated grains	Pleistocene
16. 726A 8X 2 50-51 cm	clay	white (copronodule)	mostly unphosphatized planktonics	Pliocene
17. 726A 8X 2 60-62 cm	clay	light brown (0.5 cm) & brown (0.5 cm)	bones fr., gypsum, few micronodules	Pliocene
18. 726A 8X 5 121-123 cm	silty sand	light brown (0.3 cm)	phos. sand with bone fr., micronodules & few planktonics	Pliocene
19. 726A 8X 7 5-7 cm	clay	light brown (0.5 cm) & brown (0.5 cm)	phos. sand with bone fr., phos. foraminifers & micronodules	Pliocene
20. 726A 9X 1 121-123 cm	sand	light brown (0.5cm) microconglomeratic	phos. sand with bone fr., micronodules & some phos. grains	Pliocene
21. 726A 9X 2 51-53 cm	sand	light brown (0.5 cm) microconglomeratic	phos. sand with bone fr.,micronodules, planktonics, benthics, coprolites & coated grains	Pliocene
22. 726A 9X 2 70-72 cm	sand	light brown (1 cm) microconglomeratic	phosphatic sand with bone fr., planktonics, benthics & coprolites	Pliocene
23. 726A 9X 3 111-112 cm	sand	—————	mostly unphosphatized planktonics, micronodules, bone fr., pellets & few phos. forams.	Pliocene
24. 726A 11X 2 57-59 cm	sand	—————	phos. sand with bone fr., pellets & spherical grains	Upper Miocene
25. 726A 12X CC 4-6 cm	sand	—————	unphos. and phos. planktonics, few bone fr.	Miocene
26. 726A 17X CC 1-3 cm	sand	—————	limestone sediments with few phosphate grains	Miocene
27. 729A 4R 4 131-133 cm	clay	—————	keels of foraminifers & glaucony grains	Pleistocene
28. 730A 2H 4 143-145 cm	sand	—————	planktonics & glaucony grains	Pleistocene
29. 730A 2H 5 52-54 cm	sand	—————	planktonics & glaucony grains	Pleistocene
30. 731A 39X 2 127-129 cm	clay	—————	mica	Miocene
31. 731A 39X 2 130-132 cm	clay	—————	mica	Miocene
32. 731A 39X 4 14-18 cm	clay	—————	mica	Miocene

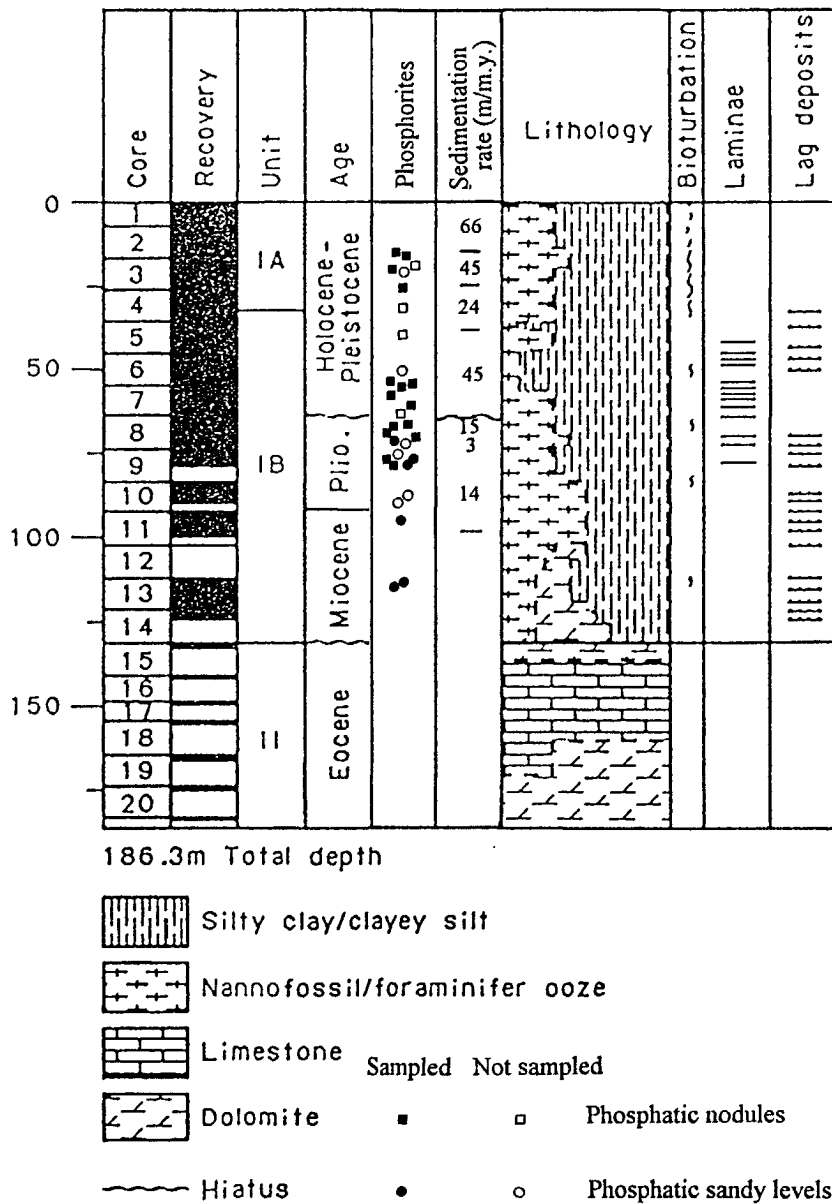


Figure 2

Lithostratigraphy of site 726 and location of phosphorite samples studied (modified after Prell et al., 1989).

RESULTS

Distribution of phosphorite nodules and phosphatic sediments

Textural studies on phosphorite levels show that certain levels (Tab. 1) are sandy, while the others vary from clayey sand to clayey. Coarse fraction studies (Tab. 1) indicate that the sediments can be broadly classified into two types: sediment levels dominated by phosphate grains, and sediment levels composed mainly of non-phosphatic grains. The former are similar to P-phosphates from the Peru margin (Garrison and Kastner, 1990) and also contain white to light-brown and a few brown nodules at some levels (Tab. 1). Sediment levels poor in phosphatic grains contain mainly planktonic and benthic

foraminifers (non-phosphatized) and several brown to dark-brown nodules at certain levels. The phosphate grains are micronodules, pellets, spherical grains, coated grains, coprolites, phosphatized foraminifers and bone fragments. The nature and relative abundance of particular phosphatic grains sometimes vary with the type of sediments: for example, micronodule abundance coincides with clay-dominated sediments and the abundance of faecal pellets which show shiny surfaces occurs at several sandy levels (Tab. 1). At site 726, 20 sediment levels were studied, 11 of which are of Upper Miocene and Pliocene age and nine are of Pleistocene age. P-phosphate sediment levels occur at six levels in Miocene and Pliocene and at two levels in Pleistocene age. P-phosphate levels occur at very close levels, sometimes separated by only a few centimetres. These observations are consistent with those reported in the Leg 117 Initial Reports.

## Petrology of nodules and micronodules

### Phosphorite nodules

The broken surface of many nodules exhibits a structure which is porous at the centre and more compact at the periphery (Fig. 3a). White to light-brown, brown and dark-brown nodule types were identified. The white to light-brown nodules are 5 to 10 mm in size, somewhat flat to irregular, and abundant in Pliocene levels. They are very porous and contain foraminifers, silt-sized detrital particles and sometimes phosphatic particles (Fig. 3b). The constituents vary from very rare to abundant from one nodule to another. These are similar to F-phosphates described from the Peru margin (Garrison and Kastner, 1990; Lamboy, 1994). Apatite occurs as interstitial cements and as a replacement of carbonate detritals. The matrix consists of ovoid to rod-shaped apatite microparticles (Fig. 3c) and inframicro and micron-sized globules, similar to phosphatized bacterial cells reported elsewhere (O'Brien *et al.*, 1981; Rao and Nair, 1988; Lamboy, 1990a and b, 1992). Frequently, ovoid-type apatite particles form rosettes or are flattened on the surfaces of skeletal particles (Fig. 3d). Deformed and hollow, rod-shaped apatite microparticles are also present (Fig. 3e). Apatitic compact nanostructures are rare. Neither dolomite nor pyrite occur in these nodules.

Brown nodules (5 mm size) are relatively compact and occur in Pliocene-Pleistocene levels. Foraminifers are the abundant constituents in some nodules and silt-sized siliclastic fragments in others (Fig. 3f). Interstitial apatite cements are most common. Porous areas show a variety of apatite particles. Ovoid to rod-shaped apatite microparticles 1-4  $\mu\text{m}$  long are the most common. Sometimes, these particles adhere to curved films and seem to have emerged from the replacement of the initial sediment component, interpreted here as most probably consisting of organic matter (Fig. 3h). Dumbbell-type (Fig. 3g) apatite microparticles also occur in these nodules. Botryoid-type apatite cements (Fig. 3j) which are anisotropic in thin section occur in some other nodules. The botryoids are about 10 to 20  $\mu\text{m}$  in diameter and formed by the aggregation of micron-sized globular apatite microparticles; they resemble botryoids reported by Br  h  ret (1991) and also the cauliflower-like microspheres of apatite, synthesized in the laboratory by microbial mediation (Lucas and Pr  v  t, 1985). Moreover, these nodules contain phosphatic tubules, about 1 m in diameter with a central cavity of about 0.3  $\mu\text{m}$ , oriented perpendicular to the surface (Fig. 3i), and may represent phosphatized microbial structures. The interstices are sometimes occupied by prismatic casts. The prisms can be seen as forming rosettes measuring some 8  $\mu\text{m}$  diameter in cross-section and composed of 1  $\mu\text{m}$ -size ovoid-type apatite particles aggregated around a nucleus (Fig. 3k). Authigenic dolomite occurs within the cavities (Fig. 4a). Bundles of fibrous clays corresponding to Mg-rich clay minerals are found in both compact and porous areas (Fig. 4c).

Dark-brown nodules are irregular, hard and dense, with shiny surfaces and between 5 and 20 mm in size. These are similar to D-phosphates of Garrison and Kastner (1990). The constituents in the nodules are similar to those in the

coarse fraction of the associated sediments (Tab. 1). This suggests an *in situ* origin. Interstitial cements are typically compact and the corresponding apatite structures under SEM seem to be a thick coalescence of globular phosphate (Fig. 3l). These globules agglomerate into small microspheres or bigger globose forms similar to botryoids (Fig. 3m). The apatite globules exhibit well-defined crystal morphologies of carbonate fluorapatite (Fig. 3n), similar to those reported by Mullins and Rasch (1985), Garrison and Kastner (1990) and Br  h  ret (1991). The crystals are intergrown, and rounded edges of the prisms can still be discerned (Fig. 3o). Microspheres exhibit a radial fibrous structure in cross section (Fig. 3o) similar to the microspheres synthesized in the laboratory (Lucas and Pr  v  t, 1984, 1985). Apatite rim cements are also present. Elsewhere, the compact apatite structure corresponds to the coalescence of small ovoids and globules (Fig. 3p). Dolomite crystals and Mg-rich clays are frequently associated with rod-shaped apatite particles (Fig. 4b and 4d). Pyrite octoids on the surfaces of globular apatite particles and pyrite framboids are admixed with rod-shaped apatite microparticles (Fig. 4e), suggesting that pyrite formation occurred immediately after and/or contemporaneously with apatite.

### Micronodules

Micronodules are about 0.5-2.0 mm size irregular grains; some show brown shiny phosphate protuberances (Fig. 5a and 5b) and others show smooth surfaces. The depressions between protuberances are filled with coccoliths molded by apatite microparticles (Fig. 5c). Micronodules show a compact internal structure with variable quantities of siliclastic and biogenic particles (Fig. 5d). Ovoid to rod-shaped apatite microparticles and pyrite framboids are found in the porous areas. The internal part of the micronodules is similar to that of the dark-brown nodules (Fig. 5e).

## Petrology of copronodules and coprolites

### Soft copronodules

White to light-brown semi-consolidated flattened bodies about 10 mm in length and 5 mm in width, associated with clayey sediments (Fig. 6a), occur on sites 725 and 726 (Tab. 1). They exhibit a homogeneous and porous microstructure (Fig. 6b). Infra-micron to micron-size globular apatite particles make up small agglomerates ranging in size from 1 to 4  $\mu\text{m}$  (Fig. 6c and 6d). Similar light-coloured, flattened to ellipsoidal phosphate bodies were reported in diatomaceous muds of the Peru margin cores (*see* Fig. 3 and 4 in Garrison and Kastner, 1990) whose microstructures (Lamboy, 1994) are identical to those reported here. These phosphate bodies are described as copronodules (Lamboy, 1994).

### Sand-sized and other hard coprolites

Sand-sized elongated phosphate particles occur in many sandy levels. Some of them show transversal constrictions

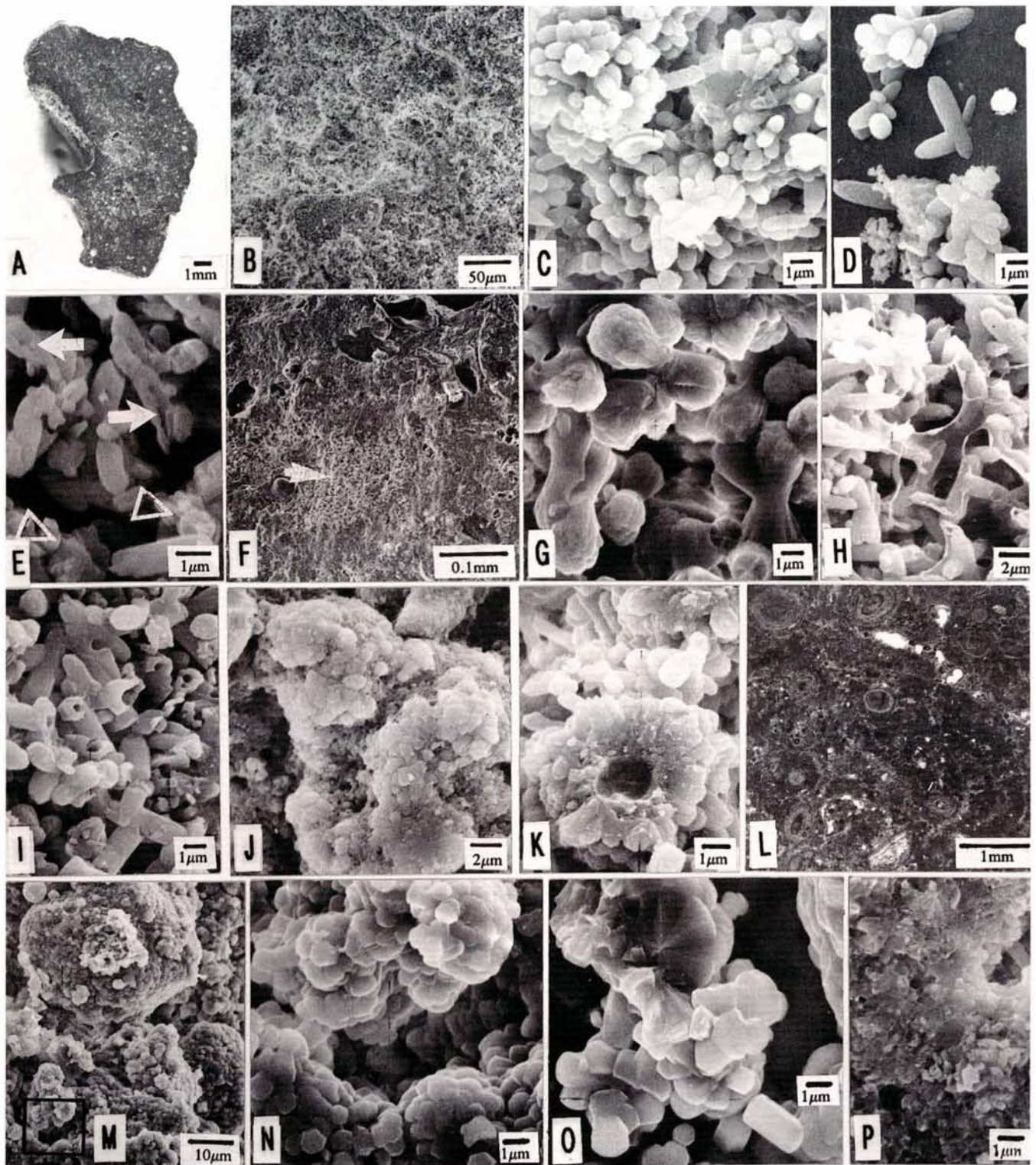


Figure 3

(a) General view of the broken surface of a nodule. (b-e) SEM photographs of white to light-brown nodules (726a, 9X, 121-123 cm); (b) at low magnification showing porous structure and faint outlines of moulds; (c) at high magnification showing aggregates of globular and rod-shaped apatite microparticles admixed with coccoliths; (d) inframicro to 4 µm sized apatite microparticles on the surface of the detrital particles; (e) deformed morphologies of apatite microparticles which show either compact (empty arrows) or hollow (full arrows) internal structure in another nodule; (f-k) SEM photographs of brown nodules (724a, 5h, 6, 65-71 cm); (f) at low magnification showing detrital particles and both porous and compact areas; (g) detail of 'F' in porous area (arrow) showing dumbbell-shaped apatite microparticles; (h) detail of porous area in another nodule showing that the rod-shaped apatite microparticles adhere to curved films; (i) the rod-shaped apatite microparticles admixed with hollow phosphatic tubules; (j) botryoid-type cement in another nodule (724b, 5h, 2, 142-143 cm); (k) prismatic casts showing aggregated ovoid type particles around a small nucleus which subsequently dissolved; (l-p) Dark-brown nodules (725a, 7x, 6, 26-28 cm): (l) thin section photograph showing abundant phosphatic coated grains and a few detrital particles in a compact matrix; (m-p) SEM photographs; (m) structure of the matrix (seen as compact at low magnification) composed of botryoids and small microspheres which are anisotropic in thin section; (n) detail of 'M' showing the crystalline aspect of globule aggregates; (o) a microsphere showing radial fibrous internal structure and prismatic apatite microparticles; (p) compact structure in another nodule (726a, 2H, 6, 78-79 cm) showing compact apatite matrix and rod-shaped apatite microparticles in porous areas.

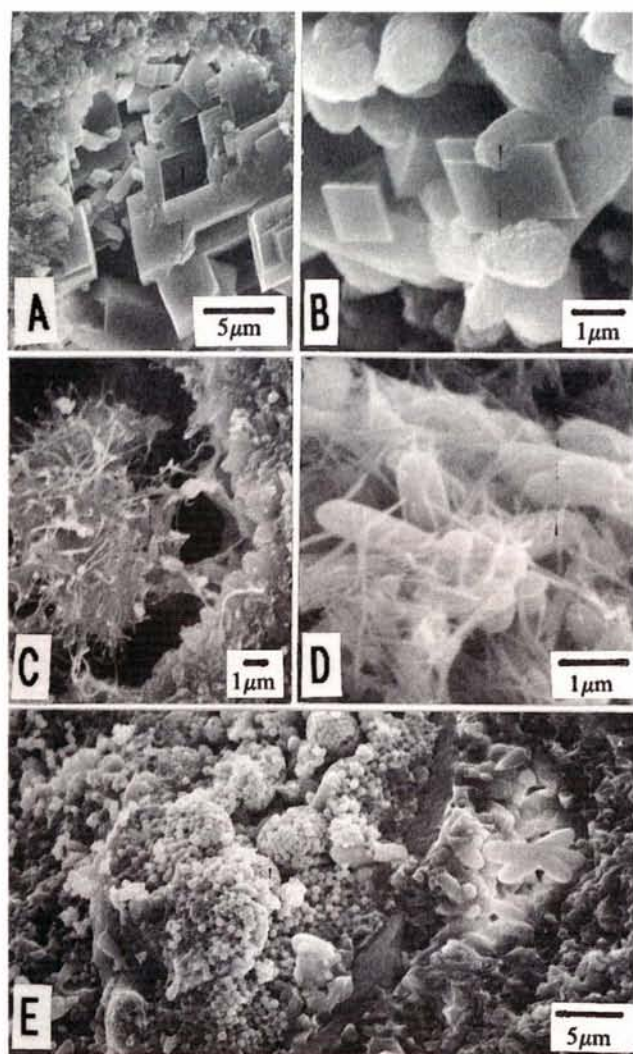


Figure 4

Other authigenic/diagenetic minerals in brown and dark brown nodules: (a) and (b) showing the dolomite crystals formed after apatite ovoids in porous areas; (c) Mg-clays in a cavity; and (d) their association with apatite microparticles; these clays appear authigenic; (e) pyrite framboids together with apatite microparticles.

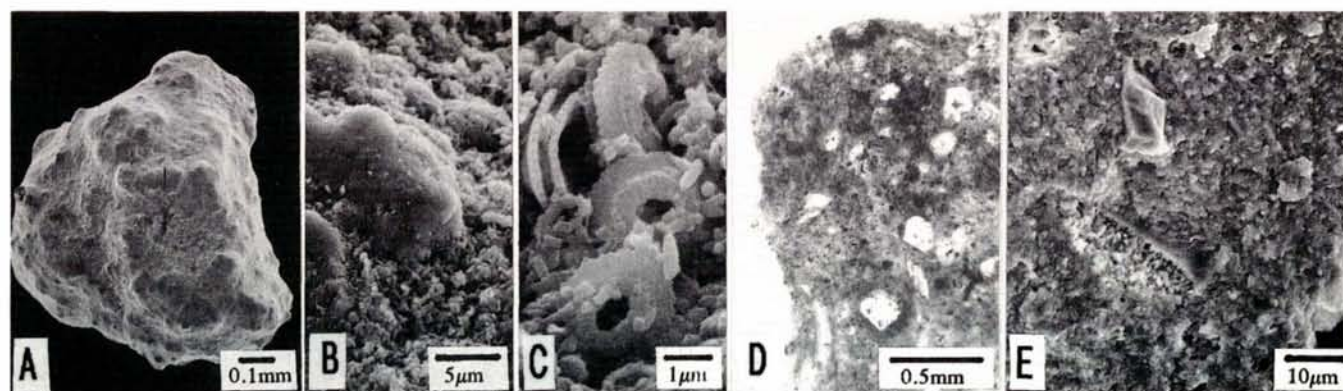


Figure 5

Micronodules (726a, 7x, 6, 26-28 cm) (a-c) SEM photographs; (a) external morphology of a micronodule; (b) detail of protuberances showing their compact aspect (c) photograph from a depression between two protuberances, showing that coccoliths are being moulded by apatite microparticles; (d) thin section micrograph of another micronodule, showing the presence of several detrital particles cemented by apatite cement; (e) the broken surface of a micronodule (726a, 8x, 7, 5-7 cm) showing predominantly compact structures; note that the peripheral portions are more compact and dense compared to the central portions.

tions (Fig. 7a), similar to the indurated excrements. They exhibit a homogeneous structure (Fig. 7b), with canals parallel to the elongation (Fig. 7c). Compact nanostructures consisting of circular to elongated pores (Fig. 7d-e) and contorted cavities are characteristic of several particles.

Phosphorite sandy levels seldom contain microconglomerate-type nodules. In one nodule, a grey-coloured particle, some 10 mm long and 5 mm thick, is cemented together with sand-sized phosphatic grains (Fig. 8a). This grey particle is homogeneous and other phosphate grains comprise peloids, coated grains and small coprolites (described below). The grey particle reveals a compact structure with many small pores and contorted cavities and is similar to the microstructure shown in Fig. 7d-e. The pores contain cell-like apatite microparticles 2 to 4 µm in diameter, displaying a granular surface texture (Fig. 8b), and are identical to the microspheres reported by Bréhéret (1991). These microspheres, which sometimes agglomerate into botryoids, display internally a spherulitic structure (Fig. 8c) which is apparently formed by radial aggregation of < 1 µm size elongate apatite crystals to a small nucleus. Imbricated microspherulitic units (Fig. 8d) occur in the adjacent compact area.

Another grain cemented with the grey particle (Fig. 8a) also displays a homogeneous aspect (Fig. 8e) and tends to be compact at the periphery and porous in its central part. Spherical cavities of variable size (< 2 mm diameter) are typical (Fig. 8f-g); some are filled with secondary apatite growth (Fig. 8f). A similar nanostructure was reported in deep-sea polymetallic nodules (Janin and Bignot, 1983), in Negev phosphorites (Soudry, 1992), in coprolites of the Peru margin (Lamboy, 1994) and in several other phosphorites (Lamboy *et al.*, 1994). Several irregular sand-sized phosphate grains at other levels also show a homogeneous nanostructure which is either porous with characteristic hollow thick walled globules (Fig. 8h) or largely compact with apatite botryoids in the pores. The compact structure also shows spherical cavities and globular apatite infillings (Fig. 8i).

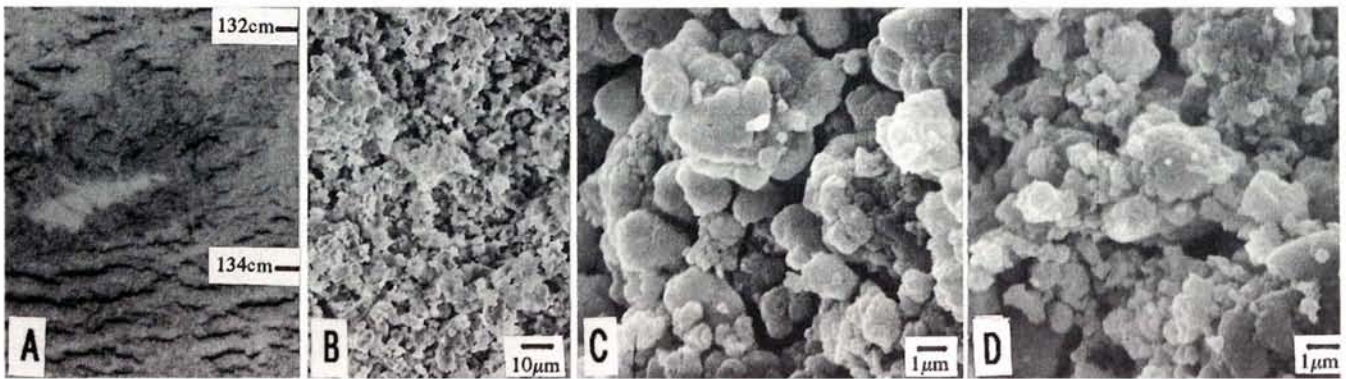


Figure 6

Soft copronodule. (a) photograph showing a white soft copronodule in a core (725c, 11x, 1, 132-135 cm). (b) low magnification SEM photograph of the broken surfaces showing the porous and homogeneous aspect; (c) and (d) high magnification SEM photographs of a nodule in Fig. 5a and in another nodule (726a, 8x, 2, 49-51 cm) showing the nanostructure comprising an aggregation of inframicro to micron-sized apatite microparticles.

### Petrology of phosphate grains

#### Pellets

White to light-brown rough-surface-textured dull pellets and brown smooth-surface-textured shiny pellets (Fig. 9a-b) were identified at several sediment levels. Thin sections (Fig. 9c) show variable content of detrital particles and porous to compact interstitial cements. White to light-brown pellets are more porous and contain some heterogeneous detrital particles (Fig. 9d). Compact apatite structures increase and detrital particle content decreases in brown pellets (Fig. 9f). Some other shiny brown pellets are predominantly homogeneous and compact (Fig. 9h). Ovoid to rod-shaped apatite microparticles (Fig. 9g), sometimes admixed with inframicro-sized apatite microparticles (Fig. 9e) are common in porous areas. The compact structure sometimes appeared to be composed of coalesced ovoid-type apatite microparticles (Fig. 9h).

#### Spherical grains

The size of the spherical phosphate grains is about 0.6 mm, approximately equal to the test size of *Orbulina*. The grains sometimes contain part of the original test and phosphatic internal mould (Fig. 10a). The diameter of the phosphatic mouldings (Fig. 10b) is comparable to the diameter of the pores of *Orbulina* tests (Fig. 10c), suggesting that the spherical grains probably represent phosphatic moulds of *Orbulina*. These grains are heterogeneous and show isotropic and anisotropic apatite cements. Similar spherical and ellipsoidal phosphatic moulds of benthic foraminifera were reported on the Peru margin (Manheim *et al.*, 1975).

The brown spherical grains generally display a compact structure (Fig. 10d). The peripheral portion of some grains under high magnification (Fig. 10e) shows that the original calcitic test is most probably replaced by apatite. Brown shiny spherical grains are more compact with a few detri-

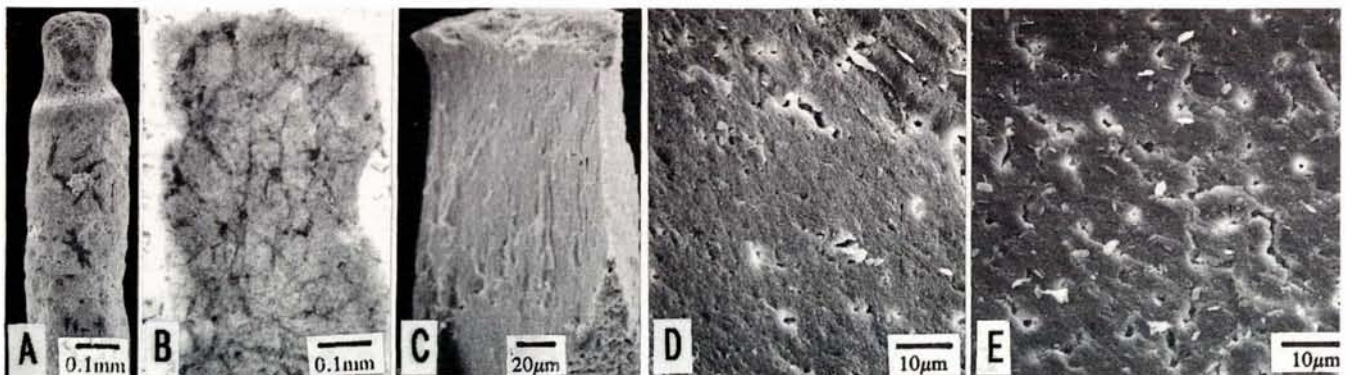


Figure 7

Hard sand-sized coprolites (726a, 6h 6, 12-14 cm). (a) SEM photograph: the surface aspect of a small elongated coprolite; (b) thin section showing the homogeneous nature; (c-e) SEM photographs (c) broken surface of a rod-shaped coprolite showing canals parallel to the elongation; (d) and (e) characteristic features of two other coprolites showing homogeneous nature and compact structure with small circular to elongated pores and contorted cavities.

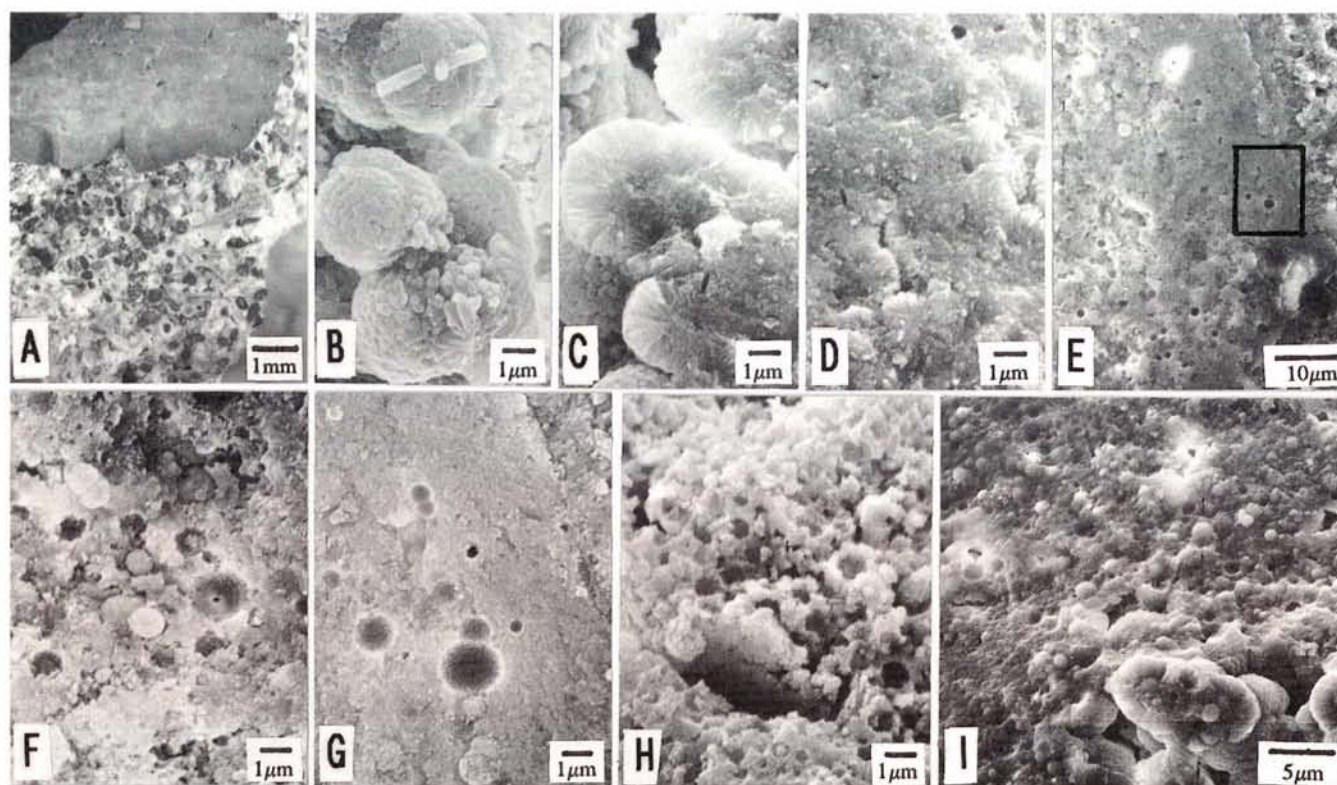


Figure 8

(a) Polished section of part of a microconglomeratic nodule (726a, 9x, 2, 66-74 cm) showing a grey big coprolite cemented to the phosphatic sand-sized grains; (b) high magnification in the porous area of the coprolite showing microspheres with a granular surface texture which agglomerate into botryoids; (c) section of microspheres showing spherulitic structure; (d) compact part showing imbricated spherulitic structure; (e-g) SEM photographs of another small coprolite cemented with phosphatic grains in the same microconglomeratic nodule: (e) a part of the coprolite showing homogeneous aspect which is compact at the periphery and porous in the centre; (f) at central part showing porous nature and more spherical cavities and cavity filled globules; (g) at the compact part showing spherical cavities and cavity filled globules; (h) nanostructure of a light-brown coprolite fragment showing hollow thick walled globules; (i) microstructure of another coprolite showing spherulitic structures; the adjacent compact structure is composed of spherical cavities and cavity filled apatite globules.

tal particles. Porous areas show either ovoid to rod-shaped or botryoid-type apatite microparticles. Compact structures are composed of tightly packed ovoids (Fig. 10f) or botryoid (Fig. 10g) type apatite particles. As pellets, some spherical grains also show morphological modifications by secondary phosphate coating (Fig. 10h).

#### Infilled foraminifers

Polished sections of the phosphatized foraminifers indicate that some chambers are filled with apatite while others are empty (Fig. 11a). If the foraminiferal chambers are empty or partly filled with sediment, the apatite microstructure is porous and consists of an admixture of ovoid and botryoid-type apatite microparticles (Fig. 11b), or micron-sized globules cluster into botryoids (Fig. 11c and 12g). This type of apatite filled foraminifers is found at many levels and also reported in other phosphorites (Lamboy and Monty, 1987; Soudry and Lewy, 1988; Lamboy, 1990a and b; Rao and Burnett, 1990). If the chambers are filled with initial sediments, the apatite structure is compact with few recognizable apatite microparticles (Fig. 11d).

#### Coated grains

Foraminifers and ovoid to ellipsoidal apatite grains are coated by phosphate. In light-brown grains, both the nucleus and cortex are porous and homogeneous (Fig. 12a) and consist of inframicro-sized apatite microparticles (Fig. 12b). The phosphatic coating is mostly compact in brown grains and its thickness varies (Fig. 12c-d). One grain was broken into two halves. A thin section made of half a grain shows no nucleus in the centre, laminated coating in the peripheral parts and dark patches distributed within the laminations (Fig. 12d). Under SEM, the other half of the grain exhibits thick compact structure containing a few porous areas around a small nucleus and discrete laminations with or without small cavities (Fig. 12e-f). The translucent and limpid aspect observed in thin section can be correlated to more compact laminations, and the black dots observed in thin section can be correlated to the small cavities; these observations are in agreement with Fikri *et al.* (1989). Some coated foraminifers are completely compact. The phosphatic coating located close to the chamber wall exhibits a spongy texture (Fig. 12g-h) which passes into compact areas. Under high magnification, these spongy textured areas are seen as 1-3 µm diameter-sized interlocked hollow structures

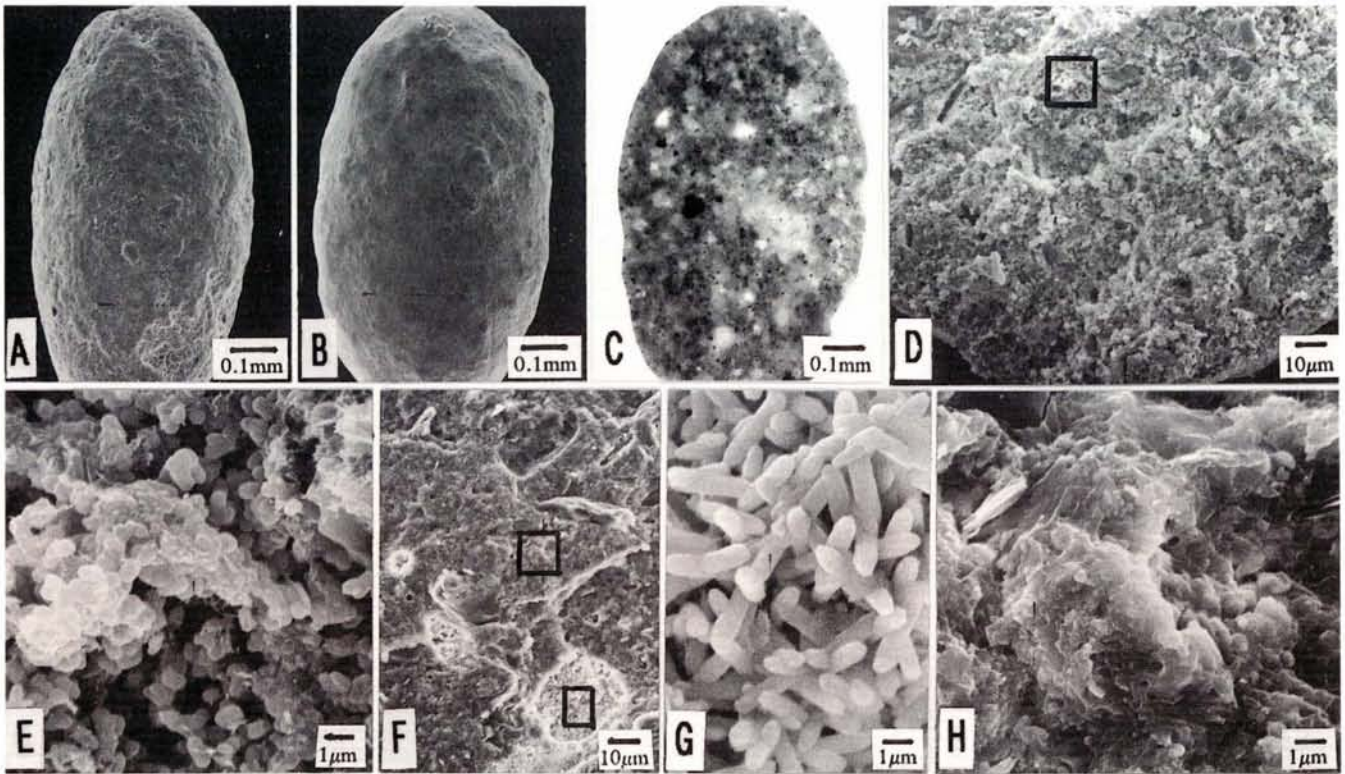


Figure 9

Phosphatized pellets (726a, 6h, 6, 12-14 cm): (a) light-brown dull pellet with heterogenous rough surface texture; (b) brown pellet with homogeneous smooth surface texture; (c) thin section photograph showing detrital particles in a phosphatic matrix; (d-h) SEM photographs - (d) broken surface of a light brown pellet showing porous and heterogeneous nature; (e) detail of 'D', apatite ovoids and globules in a porous area; (f) broken surface of a brown pellet showing more compact and few porous areas; (g) detail of 'F', showing well developed ovoid to rod-shaped apatite microparticles; (h) detail of 'F' compact structure.

(Fig. 12h). The wall separating the hollow structures is made up of submicron-sized particles. This honeycomb pattern is identical to the polyhedral cell units described by Soudry and Lewy (1990) in Negev phosphorites and by Lamboy (1994) in Peru phosphorites.

#### Bone fragments

Bone fragments are very common in phosphatic levels and also occur in nodules and micronodules. They can be recognized by their morphology under a binocular microscope or by their anisotropic apatite in thin section. Under SEM, they show a compact or spongy structure.

#### Mineralogy and geochemistry

X-ray diffraction studies on phosphorite nodules and several types of phosphate grains indicate that carbonate fluorapatite (CFA) is the most abundant mineral, followed by calcite, in all the samples. In addition, quartz and Mg-clays are present in light-brown nodules; quartz, Mg-clays and dolomite are present in brown nodules; and quartz, Mg-clays, dolomite and pyrite are present in dark-brown nodules. Pyrite is also present in micronodules. CFA and calcite are the only mineral phases in shiny pellets and coprolites. All the apatite peaks are sharp and strongly crystalline. The structural  $\text{CO}_2$  content of CFA is high,

varying from 4.6 to 5.9 %; these values are similar to those reported in replacement type diagenetic phosphorites from other areas (Parker, 1975; Birch, 1980; Rao and Burnett, 1990). The 'a' cell dimensions in our phosphorites are low and range from 9.325 to 9.33 Å indicating the high  $\text{CO}_3$  substitution as based on results of McClellan and Lehr (1969) ( $\text{CO}_3:\text{PO}_4$  ratio varies from 0.21 to 0.25).

SEM-tied-EDS analyses (78 points) indicate that all the apatite microparticles described here contain a high content of phosphorus.  $\text{TiO}_2$  and  $\text{MnO}$  were detected at only four points and the values range from 0.01 to 0.09 wt% and 0.03 to 0.06 wt%, respectively. Iron content is low and was not detected at 27 points (out of 78). The  $\text{P}_2\text{O}_5$  content ranges from 21 to 35%. Whitish phosphate pellets and some coated grains consisting of abundant detrital particles showed high contents of Si, Al, Mg, Na, S and less P; others which contain less detritals showed high P contents. The  $\text{P}_2\text{O}_5$  content of the apatite microparticles located in porous areas varied widely, probably due to the shifting of the electron beam and thus the adjacent matrix composition may have been included in the analysis. The variation of  $\text{P}_2\text{O}_5$  and CaO in the compact structures of different particles is within the range of 3% (Tab. 2). The CaO/ $\text{P}_2\text{O}_5$  values in the compact structures range from 1.58 to 1.75, which are higher than the pure carbonate fluorapatite (1.54, McClellan and Lehr, 1969). Although EDS and microprobe results are not comparable, in order to find out the relative and apparent variations of elements,

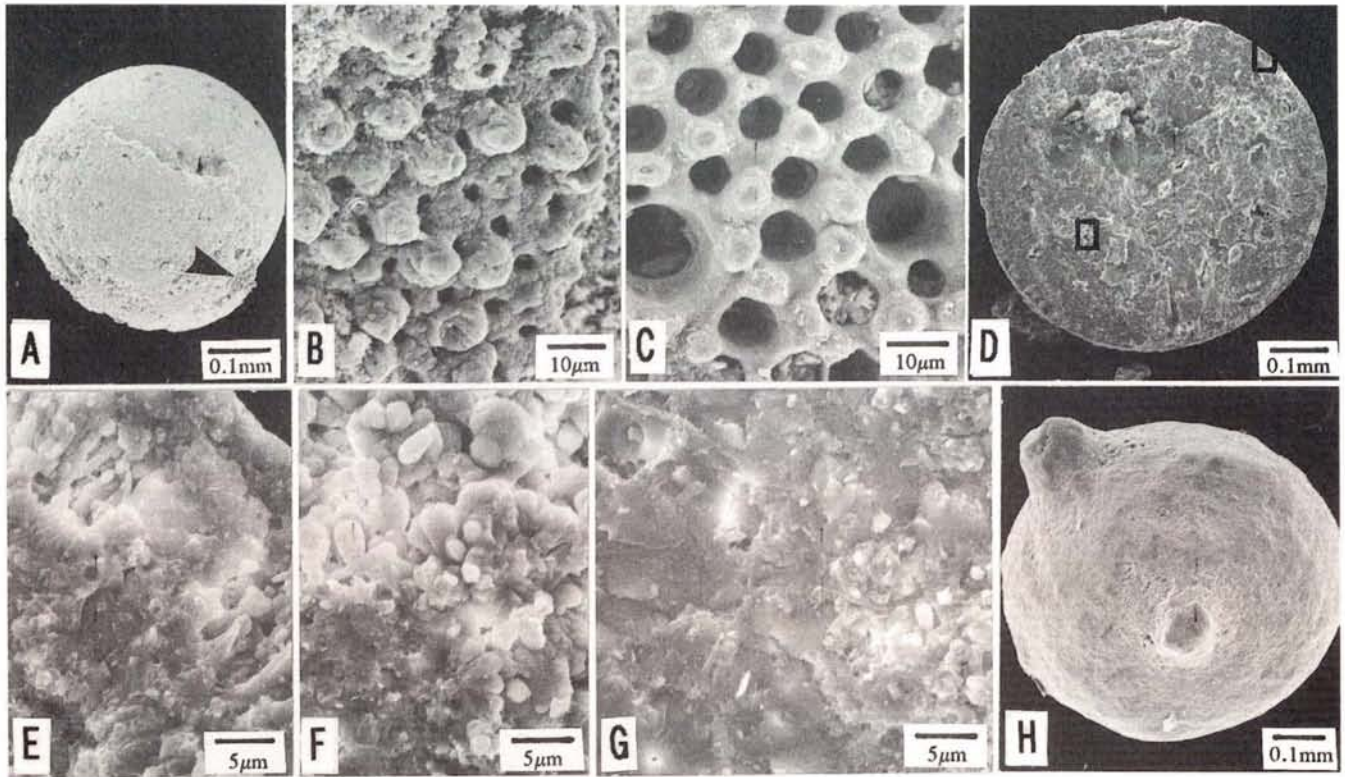


Figure 10

Spherical grains (726a, 11x, 2, 57-59 cm). (a) rough surface textured grain showing phosphatic internal mould on the upper portion and part of the original test on the lower portion; (b) detail of 'A' (black arrow) after rotation showing the phosphatized part of the original test, probably *Orbulina*; (c) external appearance of non-phosphatized *Orbulina* test showing the characteristic presence of two sizes of pores; (d) broken surface of a grain (SEM photograph); (e) detail of a grain at the peripheral part showing the apatite formation most probably by replacement; (f) showing ovoid to rod-shaped apatite microparticles in porous and compact areas; (g) compact apatite structure corresponding to coalesced botryoids; (h) shiny spherical grain showing protuberances.

the compact structures analysed in this study were compared with the phosphatic matrix in nodules from other regions. Our phosphorites are enriched in Na, Al, Ca, Mg, K, P and S and poor in Fe when compared with microprobe analyses of phosphorites reported by Glenn and Arthur (1988) and Piper *et al.* (1988) on the Peru margin. Similarly, our phosphorites

contain higher Na, Ca, P, S and lower K, Si, Fe and Al than the non-ferruginous phosphatic nodules of the East Australian continental margin (O'Brien *et al.*, 1990). The contrasting differences in the concentrations of the elements are most probably due to the abundance of Mg-rich clays and the absence of glauconite in Oman margin phosphorites.

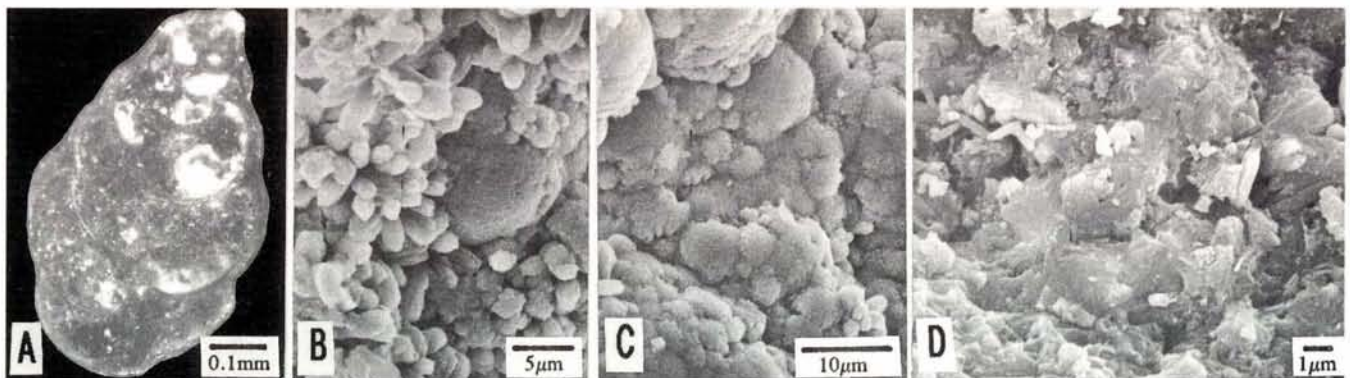


Figure 11

Phosphate infilled foraminifers (726a, 9X, 2, 51-53 cm). (a) polished section showing that some chambers are empty and the others filled with phosphate matrix; (b-d) SEM photographs; (b) ovoid to rod-shaped and botryoid apatite microparticles in empty chambers; (c) apatite botryoids in partly sediment filled chambers; (d) compact apatite structure in a completely filled phosphatized foraminiferal chamber showing coalesced botryoids and rod-shaped particles.

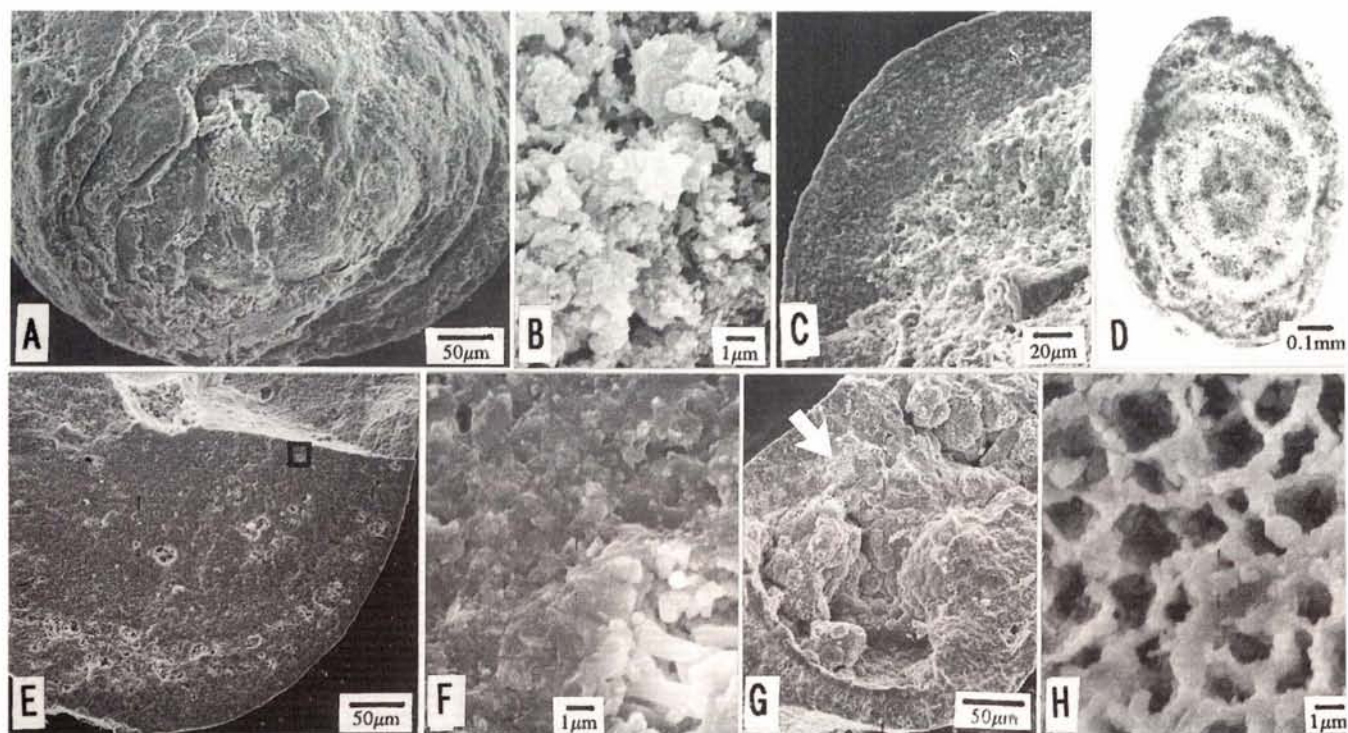


Figure 12

Coated grains (726a, 7x, 6, 26-28 cm). (a) white grain showing several phosphatic coatings; (b) broken surface of the same grain showing laminations and porous structure; (c) grain showing compact brown phosphatic coating at the peripheral parts and heterogeneity in the centre; (d) thin section photomicrographs of a coated grain; (e) SEM photograph of the same grain: many black dots in some coatings observed in 'D' correspond to small cavities and the limpid aspect of other coatings in thin section correspond to very compact apatite structure; (f) detail of 'E' compact structure and apatite microparticles in a small cavity; (g) another coated foraminifer (726a, 9x 2, 51-53 cm) showing apatite infillings in test chambers and compact phosphatic coating; (h) detail of 'G' white arrow showing polyhedral cell units of apatite.

## DISCUSSION

### Phosphate evolution with in the phosphorite macroparticles

Bone fragments are initially phosphatic. The origin of some coated grains is not very clear. The external morphology of all other macroparticles, such as coprolites, pellets, spherical grains and nodules, was largely preserved. The porous/compact internal structure varies from one particle to the other and seems to be related to the degree of phosphatization within the particle. It appears that phosphatization took place within the initial supports and that the evolution of phosphate therein is related to the development of apatite microparticles and non-apatitic components, and to the macroscopic character of phosphate particles.

#### The main type of apatite microparticles

Ovoid to rod-like apatite particles are the most common and occur in almost all types of phosphorite particles. Similar types of particles were reported in several other phosphorites and considered as phosphatized bacterial cells (O'Brien *et al.*, 1981; Rao and Nair, 1988; Soudry and Lewy, 1988; Lamboy, 1990a-b, 1994). The deformed and hollow rod-shaped microparticles (Fig. 3e) may have

resulted from the phosphatization of the external organic sheath of the bacterial bodies and thus support microbial origin. It would be difficult to explain their formation by inorganic chemical precipitation.

Botryoids formed by the agglomeration of microspheres (Fig. 8b-11l) or coalescence of globular apatite microparticles (Fig. 3j, 3m-n) are common in many nodules and grains. The spherulitic (Fig. 8c) or radial fibrous internal structure (Fig. 3o) of these particles and imbricated spherulitic structures in the adjacent compact part (Fig. 7e, 8d, 8i) may suggest that the particles represent phosphatized microbes which were densely packed in the compact areas. Monty (1976) reported spherulites grown within the hollow shells of organic matter and spherulites showing a compromised imbricated structure beneath a microfilamentous bacterial film. Aragonite spherulites and phosphatized microspheres showing radial fibrous structures were produced under laboratory conditions by bacterial action (Krumbein, 1979; Lucas and Prévôt, 1985). Several workers reported botryoids (Lamboy and Monty, 1987; Soudry and Lewy, 1988; Lamboy, 1992, 1993) and others spherulites (Soudry and Lewy, 1988) in phosphorites and suggested that the former represent phosphatized microbial remnants and that the latter were formed by microbial influence. Dumbbell-like apatite particles are rare in our samples (Fig. 3g). Dumbbells formed by bacterially induced precipitation of calcium carbonate were produced in

Table 2

Average composition of the compact apatitic structures in nodules and grains.

element	nodules (4)*	forams (4)*	moulded areas (2)*	coprolites (4)*
Na <sub>2</sub> O	2.69	1.99	2.96	1.93
MgO	2.10	1.37	2.53	1.12
Al <sub>2</sub> O <sub>3</sub>	2.51	1.00	1.76	0.90
SiO <sub>2</sub>	3.62	2.51	2.82	1.99
	min 31.81	30.32	31.92	28.59
P <sub>2</sub> O <sub>5</sub>	32.51	31.98	32.99	32.05
	max 33.16	32.45	34.04	33.98
SO <sub>3</sub>	3.93	4.52	4.36	4.24
K <sub>2</sub> O	0.59	0.46	0.60	0.46
	min. 49.21	55.25	50.62	50.78
CaO	51.61	56.06	51.96	57.28
	max. 54.63	60.82	53.31	63.53
FeO	0.20	0.13	0	0
CaO/P <sub>2</sub> O <sub>5</sub>	1.59	1.75	1.58	1.78

\* number of spots analysed.

the laboratory (Buczynski and Chafetz, 1991). Horodyski and Vonder Haar (1975) reported polyhedral structures, similar to those reported here (Fig. 12h), in calcified algal mats, and interpreted them as remnants of cellular material of *Entophysalis* colonies. Dexter-Dyer *et al.* (1984) suggested that the mat assemblages often leave hollow structures after death and that these hollow structures can be preserved in the rock if there is no intense diagenesis. Soudry and Lewy (1990) interpreted the phosphatic polyhedral cell-like units as phosphatic external moulds of subsequently dissolved micritic particles. Since microbial communities can be colonized on any hard surface in sediments (Gerdes and Krumbein, 1987), we propose that the phosphatic coatings, consisting of polyhedral cell units (Fig. 12h), may record local colonization of microbial cells on grain surfaces and their subsequent phosphatization.

Some coprolites display typical structures represented by hollow micron sized globules with a thick wall (Fig. 8h), spherical cavities (Fig. 8f-g) and cavity-filled globules (Fig. 8f-8i). Janin and Bignot (1983) reported similar structures in polymetallic nodules and interpreted them as external precipitation around bacteria. Similar structures were reported in phosphatized microbial mats (Soudry, 1992) and in coprolites (Lamboy, 1994) with the suggestion that these cavities correspond to the external moulding by microbial cells.

#### Evolution of apatite microparticles and apatite structures

The diagenetic evolution of the original apatite microparticles or structures is evident: (a) the crystalline aspect of some ovoids (Fig. 3n-o) and botryoid-type apatite particles (Fig. 3o); (b) the compact structures extending into the areas showing polyhedral cell units (Fig. 12g-h); (c) compact structures developed at the peripheral parts (Fig. 3a, 8e); and (d) filling of inframicro particles in spherical cavities (Fig. 8f-8i) may suggest an overgrowth of apatite.

Elsewhere, compact structures seem to correspond to densely packed ovoidal (Fig. 10f) or botryoidal (Fig. 7e, 8d, 8i) apatite particles; coalescence of apatite particles may suggest an evolution. Compact structures at the periphery in all kinds of phosphorite particles (Fig. 3a, 5d, 8e, 8g, 9h) may be a proof that evolution of apatite starts there. It seems that highly evolved particles are the most compact. Since similar types of apatite particles at the same stratigraphic level show different degrees of compactness, it is suggested that apatite overgrowth and compactness might be the consequence of chemical precipitation during early diagenesis.

#### Aspects of evolution at the scale of macroparticles

As the external morphology of the macroparticles is preserved, one may consider each initial support to have acted as a microenvironmental niche within which the apatite grew and the initial constituents were pseudomorphically replaced by apatite. Organic matter is an abundant constituent in the excrements. The initial framework of pellets, foraminiferal test infillings, micronodules and nodules is a part of the sediment which consists of mixture of clays, biogenic detritals and organic matter. Except in copronodules/ coprolites, the porous and compact structures and apatite microparticles are unevenly distributed in the matrix. This may be due to the heterogeneity of the initial framework and/or to differential speed of development of apatite controlled by the juxtaposition of areas of different microenvironmental conditions. The highly evolved particle appears more compact and homogeneous.

Mg-clays and quartz in all types of nodules are mostly detritally derived (*see* Debrabant *et al.*, 1991). Authigenic minerals (dolomite and pyrite) other than apatite are present in some nodules. The presence of dolomite and pyrite in brown and dark-brown nodules and their absence in white to light-brown nodules is roughly proportionate to the increasing compactness. The nodule containing both dolomite and pyrite may therefore be considered as diagenetically more evolved. The evolution probably depends on the residence time of the nodule in the upper centimetres of the sediment and on redox conditions within the sediment. Therefore, the presence of dolomite and pyrite in a nodule does not indicate that reducing conditions were favourable for apatite precipitation, but that the nodule remained in reducing conditions for a longer time during and after the apatite formation.

The overall mineralogical evolution of a phosphate particle is indicated by colour and compactness in all macroparticles; the more evolved particles are darker and denser, and exhibit a shiny aspect. Therefore the variation in these features in any macroparticle (nodules, pellets, spherical and coated grains) may be an index of the extent of evolution of phosphate, rather than abrasion during reworking. However, colour alone may sometimes be misleading if there is external phosphate encrustation.

It has been noted that pellets consisting of several siliclastic particles and porous apatite structures and other pellets showing homogeneity and compact apatite struc-

tures occur at different phosphatic sand levels. Since some of the coated grains exhibit a homogeneous and compact apatite structure as their nucleus, it is possible that the coated grain itself may be a faecal pellet produced by another benthic invertebrate with a different feeding system. In this process, different layers of organic matter may have developed on faecal pellets/pellet fragments which subsequently phosphatized and appear as a phosphate coated layers of different porosity (Fig. 12a-d). This explanation for coated grains is admittedly tentative and is not valid for all coated grains (for example, coated foraminifers, (Fig. 12g-h). Our studies therefore indicate that each phosphorite particle is a diagenetic rock showing different evolution steps. A phosphate grain was considered as a world by Cayeux (1950) and as complex rock by Riggs (1979). Soudry and Nathan (1980) suggested that the end product of diagenetic phosphatization of faecal pellets, aggregates, bone fragments and intraclasts is a structureless phosphate peloid.

### Environmental conditions of phosphatization

Prell *et al.* (1989) described the sediment levels dominated by phosphate grains as lag deposits which accumulated by the reworking process. The high number (50 000) of benthic foraminifers per cubic centimetre of sediment (Hermelin, 1990 and 1991), the low rate of sedimentation (15 m/my), very low Planktonic/Benthic foraminifer ratio and high bioturbation suggest that shallow oxic conditions existed during this time (Upper Miocene to Early Pliocene).

Our studies indicate that phosphatized pellets, foraminiferal tests and coprolites dominate at many intervals. The dark-brown and shiny aspect of the grains is due to diagenetic evolution rather than to reworking. Oxic and shallow water conditions at the site favour benthic activity and bioturbation which in turn lead to the production of faecal pellets and other granular substrates. Micro-environments within these smaller granular substrates probably favoured more rapid phosphatization. Burnett *et al.* (1988) reported that the pellets can phosphatize faster (in about 10 years) than nodules.

White to light-brown nodules also occur in these levels. As they are fragile, the explanation that they accumulated by reworking is not tenable. Furthermore, the nodules enclose several phosphate grains, indicating that their formation was subsequent to the grain formation. The light colour, the absence of other authigenic minerals (such as dolomite and pyrite) and the porous and friable nature of the nodules indicate that their formation, like that of phosphate grains, most probably occurred *in situ* by rapid early diagenetic processes. As low sediment accumulation rates existed at these levels, some sort of minor hardground conditions may be responsible for their formation. Burnett *et al.* (1980) reported similar types of nodules at the intersection of Oxygen Minimum Zone (OMZ) on the continental shelf/slope off Peru and Chile. Garrison and Kastner (1990) and Glenn *et al.* (1994) described these as protocrusts/soft grounds and

considered them to be the precursors of D-phosphates and hardgrounds.

Some well sorted phosphate grain-rich sediment layers are only a few millimetres thick, suggesting that no large-scale reworking was associated with them. Site 726 is located close to the shelf edge where one would expect higher intensity of gravity and internal currents. Slight winnowing caused by these currents might have accumulated these sands.

Between Late Pliocene and Early Pleistocene, the sediment levels dominated by phosphate grains decrease upwards and are replaced by brown and dark-brown phosphate nodule-rich levels interbedded with diatom-rich laminated beds that contain no phosphorites. The increase of water depth, the existence of OMZ and a relative increase in sedimentation rates (from 15 to 45 m/my, Prell *et al.*, 1989) during this period probably controlled the formation of granular frameworks such as faecal pellets and foraminifer infillings. The other constituents (detrital clays, dolomite and pyrite) in the nodules indicate that part of the sediment acted as initial support, subjected to intense diagenesis during phosphatization, and thus evolved into more and more compact nodules. The absence of nodules at other sites for the corresponding levels may be due to high sedimentation rates inhibiting the formation of nodules.

During the Late Pleistocene, phosphorites occur as some scattered micronodules to well cemented nodules. The high sedimentation rates (80-150 m/my, Prell *et al.*, 1989) may be responsible for the apparent absence of Holocene and Recent phosphorites.

### Comparison of phosphorites from the Oman and Peru margins

Physiographic settings and type of phosphorites at Oman and Peru margins are compared in Table 3. Phosphorite nodules, pellets and coprolites formed from three types of initial supports occur in both Peru and Oman margin sediments. Macroconglomerate nodules and massive or laminated phosphatic encrustings representing complex hardgrounds (Garrison and Kastner, 1990) and phosphatized bivalve shell fragments (Lamboy, 1992) occur only on the Peru margin.

Several ODP sites on the Peru margin showed numerous larger nodules and nodule-rich beds, thicker and greater number of phosphatic sandy layers. This demonstrates that these beds are the result of winnowing and reworking. In contrast, phosphorites on the Oman margin are important only at one site (726); phosphorite nodules are smaller and sparsely distributed; phosphate sand layers are only a few millimetres thick.

Intensively burrowed phosphorite levels and phosphate sand layers on both the margins indicate intermittent oxic conditions, probably resulting from a shifting of the upper boundary of the OMZ. This implies that phosphatization also occurs in oxic to suboxic conditions.

The Peru margin phosphorites are associated with diatom-rich sediments. The Oman margin phosphorites are asso-

Table 3

Comparison of physiographic settings and phosphorites from ODP cores off Oman margin and Peru margin (Source of data : Leg 117 - this paper and Prell, Niitsuma et al. (1989) ; Leg 112 - Suess, von Huene et al. (1988), Garrison & Kastner (1990) and Lamboy (1993, 1994).

Character	Leg 117 (off Oman margin)	Leg 112 (off Peru margin)
<b>1. Physiographic settings associated with phosphorites</b>		
a. shelf break	100-150 m depth	150 m depth (only at 9°S)
b. continental slope	extremely steep slope, sometimes upto 35° dip	wide terraces on upper, middle and lower slopes below 11°S
c. upwelling	intense but seasonal	intense and persistent
d. oxygen min. zone	200-1200 m depth	150-400 m depth
e. associated sediments	foram-rich calcareous	diatom-rich silicious, sometimes foram-rich
f. organic matter	marine but reworked nature	marine and lipid-rich
<b>2. Phosphorites</b>		
a. abundance	present at only three shelf & upper slope sites	abundant at all shelf slope sites
b. average size of nodules	small	frequently large
c. thickness of phos. sandy levels	about 0.5 cm	about 0.5 m
<b>3. Type of phosphorite macroparticles</b>		
a. light-coloured nodules	present	abundant
b. dark-coloured nodules	confined to Pleistocene-Holocene intervals	abundant at many intervals
c. conglomeratic nodules	rare	common
d. hardgrounds	absent	frequent
e. micronodules	abundant	less abundant
f. soft copronodules	present	present
g. coprolites	present	rare
h. phosphate grains	common	common
i. fish remains	common	common
j. phosphatized bioclasts	absent	present
<b>4. Apatite microparticles</b>		
a. ovoid to rod-shaped m.	very common	very common
b. botryoids	common, in nodules and in grains	absent in nodules but present in grains
c. dumbbell-like m.	less common, in nodules and in grains	less common, only in grains
d. micron-sized globules	frequent	frequent
e. inframicro-sized g.	frequent	frequent
f. polyedral cell units	rare	rare
<b>5. Associated minerals with phosphorites</b>		
a. glauconite	absent within phosphorites and at phosphate intervals	present at few sites in some ph. and at phosphate intervals
b. pyrite	less common	common
c. dolomite	occurs only in cavities of nodules	occurs as cement as well as dolomicrite particles or intervals
d. fibrous Mg-clays	very common	not reported

ciated with calcareous sediments. The pore waters on the Oman margin are expected to contain high carbonate ions with high alkalinities. The excess carbonate ions act as lattice poisoning ions and inhibit the precipitation of CFA (Glenn and Arthur, 1988).

Glenn and Arthur (1988) reported a paragenetic sequence of glauconite, CFA, pyrite and dolomite in the phosphorite nodules of the Peru margin. It was suggested that a Fe-redox cycling process is important in phosphorite formation. On the Oman margin, glauconite does not occur in association with phosphorite, dolomite is limited to pore cavities and formed irrespective of pyrite (note - on the Peru margin the dolomite formation is always later than pyrite formation) and pyrite is restricted to a few dark-brown nodules. These factors suggest that sulphate reducing conditions and element concentrations, especially the availability of iron in the interstitial waters, probably limited the formation of pyrite and to some extent the enrichment of P (adsorbed P on oxy-hydroxides). This may be due to the lack of terrigenous supply of metals through rivers (other than aeolian input). These findings also suggest that ferrous redox cycle phosphate pumping (Froelich *et al.*, 1988; Heggie *et al.*, 1990) was not a significant process in the formation of Oman margin phosphorites.

The organic matter on the Peru margin sediments is marine and lipid-rich with a high mean hydrogen index and low oxygen index which indicate its well preserved nature. The organic matter on the Oman margin is also marine but less labile and tends to be degraded to a significant degree as shown by high C/N ratios (Emeis *et al.*, 1991). Furthermore, the rate of sulphate reduction at the Oman shelf is significantly less than at the Peru margin and has been attributed to the nature of the organic matter (Pederson and Shimmiel, 1991). Therefore, the type and reactivity of organic matter that reaches the bottom sediments control the enrichment of interstitial P and phosphorite formation. The refractory nature of organic matter could be due to a long residence time in the water column and to a less pronounced OMZ (discussed below).

On the Peru margin, the OMZ occurs persistently between 150 and 400 m water depth. On the Oman margin, the OMZ occurs between 200 and 1200 m water depth and this water column is stratified with intermediate water masses (Red Sea and Persian Gulf waters) which are highly saline and oxic (Prell *et al.*, 1989). The severity of the OMZ depends on the inflow of Red Sea and Persian Gulf waters. Therefore, the periodic weakening of the OMZ probably affects the phosphogenesis.

Recent studies have shown hardground conditions to be important in the formation of Peru margin phosphorites (Glenn *et al.*, 1994). The high sediment accumulation rates on the Oman margin inhibit the hardground conditions.

We presume that the excess carbonate ions in the pore waters, reworked organic matter, weakened oxygen minimum zone and lack of hardgrounds are responsible for the development of phosphorites and for the apparent absence of present day phosphorites on the Oman margin.

## CONCLUSIONS

Phosphorites on the continental slope of the Oman margin are important at only one ODP site 726. Phosphatic grains dominated sandy levels with light brown nodules from Upper Miocene to Early Pliocene, and non-phosphatic grains dominated sandy and/or clayey levels with brown and dark brown nodules from Late Pliocene to Early Pleistocene are present. Phosphatic grains include coprolites, pellets, foraminifer infillings, spherical and coated grains, fish remains and micronodules.

The external and internal aspects of phosphate macroparticles indicate that phosphatization took place within the initial supports by microbial processes. The colour of the macroparticle, porosity / compacity and heterogeneity / homogeneity within the particle are reflective of the extent of evolution of the contained phosphate. It appears that the dark-brown shiny macroparticles with homogeneous compact apatite internal structure are highly evolved.

During the Miocene to Early Pliocene, the site was at shallow depths and oxic conditions existed. Bioturbation and benthic activity provided several initial substrates within which phosphatization took place. The deeper water conditions and existence of an oxygen minimum zone from Late Pliocene controlled the formation of initial supports such as faecal pellets and benthic forams; in these conditions, part of the sediment acted as initial support and microenvironments within the substrates and in associated sediments contributed for their evolution into brown and dark-brown particles.

The number and thickness of phosphatic sand layers and nodule beds are more numerous in several ODP sites of the Peru margin than on the Oman margin. Similarly, complex nodules and phosphorite crusts reflecting hard grounds are present only on the Peru margin. It appears that apart from upwelling, the nature of organic matter, the intensity of the oxygen minimum zone and the high rate of sedimentation play a role in the phosphorite formation.

## Acknowledgements

The authors thank Dr. P.A. Dupeuble, University of Rouen, for his help at various stages. Rao thanks the Department of Science and Technology (India) and the Commission of the European Communities (Brussels) for offering a post-doctoral fellowship under which this work was carried out. Rao also thanks the Director and R.R. Nair, Head Geological Oceanography Division of the National Institute of Oceanography, Goa for their encouragement. We also thank ODP staff at College Station for allowing one of us to inspect and subsample the cores. We are grateful to the anonymous reviewer for his comments which improved the manuscript. This paper is a contribution to IGCP project 325: Correlation of palaeogeography with phosphorites and other authigenic minerals.

## REFERENCES

- Baturin G.N.** (1982). Phosphorites on the ocean floor. Origin, composition and distribution. *Developments in sedimentology* **33**, Elsevier, 345 p.
- Bentor Y.K.** (1980). Phosphorites - the unsolved problems. In: *Marine Phosphorites* Y.K. Bentor, ed. SEPM sp. publ. No. **29**, 3-18.
- Birch G.F.** (1980). A model of pencontemporaneous phosphatisation by diagenesis and authigenic mechanisms from the western margin of Southern Africa. In: *Marine Phosphorites* Y.K. Bentor, ed. SEPM sp. publ. No. **29**, 79-100.
- Bréhéret J.G.** (1991). Phosphatic concretions in black facies of the Aptian - Albian marnes blues formation of the Vocontian basin (SE France) and at site DSDP 369: evidence of benthic microbial activity. *Creta. Res.* **12**, 411-435.
- Buczynski C., Chafetz H.S.** (1991). Habit of bacterially induced precipitation of calcium carbonate and the influence of medium viscosity on mineralogy. *J. Sediment. Petrol.* **61**, 226-233.
- Burnett W. C., Baker K.B., Chin P.A., McCabe W., Ditchburn R.** (1988). Uranium series and AMS <sup>14</sup>C studies of modern phosphatic pellets from Peru shelf muds. *Mar. Geol.* **80**, 215-230.
- Burnett W.C., Veeh H.H., Soutar A.** (1980). U-series, oceanographic and sedimentary evidence in support of recent formation of phosphate nodules. In: *Marine Phosphorites* Y.K. Bentor, ed. SEPM sp. publ. No. **29**, 61-71.
- Cayeux L.** (1950). Les phosphates de chaux sédimentaires de France, Etude des gîtes minéraux de la France. *Service. Carte Géol. Fr.* Paris 458 p.
- Cook P.J., McElhinny M.L.** (1979). A reevaluation of the spacial and temporal distribution of sedimentary phosphate deposits in the light of plate Tectonics. *Econ. Geol.* **74**, 315-330.
- Debrabant P., Krissek L., Bouquillon A., Chamley H.** (1991). Clay mineralogy of Neogene sediments of the western Arabian sea: Mineral abundances and paleoenvironmental implications. In: *Proc. of the Ocean Drilling Program, Scientific Results Leg 117*. Prell, W.L., Niitsuma, N. et al. eds. College Station, Tx, **117**, 183-196.
- Dexter-Dyer B., Kretzschmar M., Krumbein W.E.** (1984). Possible microbial pathways in the formation of Pre-cambrian ore deposits. *J. Geol. Soc.* London **141**, 251-262.
- Emeis K.C., Morse J.W., Mays L.L.** (1991). Organic carbon, reduced sulfur and iron in Miocene to Holocene upwelling sediments from the Oman and Benguela upwelling system. In: *Proc. Ocean Drilling program Scientific Results Leg 117*, Prell, W.L., Niitsuma, N. et al. eds. College Station, Tx, **117**, 518-528.
- Fikri A., Lamboy M., Benalioulaj S., Trichet J., Belayouni H.** (1989). Contribution à l'étude pétrologique de la matière organique dans les phosphates naturels. Nouvelles approches méthodologiques. *Bull. Soc. Géol. France* **8**, 979-987.
- Froelich P.N., Arthur M.A., Burnett W.C., Deakin M., Hensley V., Jahnke R., Kaul L., Kim K.H., Soutar A., Vathakanon C.** (1988). Early diagenesis of organic matter in Peru continental margin sediments: phosphorite precipitation. *Mar. Geol.* **80**, 309-343.
- Garrison R.E., Kastner M.** (1990). Phosphatic sediments and rocks recovered from the Peru margin during ODP Leg 112, In: *Proc. Ocean Drilling program Scientific Results Leg 112*, Suess, E., Von Huene, R. et al. eds. College Station Tx, **112**, 111-134.
- Gerdes G., Krumbein W.E.** (1987). Biolaminated deposits. *Lecture notes in Earth Sciences*, Springer-Verlag, New York-Berlin-Heidelberg. 1-183 p.
- Gevork'yon V.K., Chugunyy Y.G.** (1970). Phosphorite nodules in the bottom sediments of the Gulf of Aden. *Oceanol.* **10**, 232-241.
- Glenn C.R., Arthur M.A.** (1988). Petrology and major element geochemistry of Peru margin phosphorites and associated diagenetic minerals: authigenesis in modern organic-rich sediments. *Mar. Geol.* **80**, 231-267.
- Glenn C.R.** (1990). Depositional sequences of the Duwi, Sibâiyâ and Phosphate formations, Egypt: phosphogenesis and glauconitization in a Late Cretaceous epeiric sea. In: Notholt A.J.G. and Jarvis I. eds. *Phosphorite Research and Development, Geological Society Spec. Publ.* **52**, 205-222.
- Glenn C.R., Arthur M.A., Resig J.M., Burnett W.C., Dean W.E., Jahnke R.A.** (1994). Are modern and ancient phosphorites really so different? In: *Siliceous, phosphatic and glauconitic sediments of the Tertiary and Mesozoic* Iijima A., R.E. Garrison, A.M. Abed eds. International Sci. Publi. Zeist. 159-188.
- Gulbrandsen R.A.** (1970). Relation of carbon dioxide content of apatite of Phosphoria Formation to regional facies. Washington D.C. U.S. Geological survey Professional Paper 700-B, B9-B13.
- Heggie D.T., Skyring G.W., O'Brien G.W., Reimers C., Herczeg A., Moriarty D.J., Burnett W.C., Milnes A.R.** (1990). Organic carbon cycling and modern phosphorite formation on the East Australian continental margin: an overview. In: *Phosphorite Research and Development* Notholt A.J.G. and I. Jarvis eds. Geol. Soc. London. sp. publ., **52**, 87-117.
- Hermelin J.O.** (1991). The benthic foraminiferal faunas of sites 725, 726, and 728 (Oman Margin, Northwestern Arabian sea) In: *Proc. of Ocean Drilling Program Scientific Results Leg 117*, Prell W. L., N. Niitsuma et al. eds. **117**, College Station Tx, 55-89.
- Hermelin J.O., Shimmield G.B.** (1990). The importance of the oxygen minimum zone and sediment geochemistry in the distribution of Recent benthic foraminifera in the northwest Indian Ocean. *Mar. Geol.* **91**, 1-29.
- Horodyski R.T., Vonder Haar S.P.** (1975). Recent calcareous stromatolites from Laguna Mormona (Baja California) Mexico. *J. Sediment. Petrol.* **45**, 894-906.
- Janin M.C., Bignot G.** (1983). Microfossiles thallophtiques des concrétions polymétalliques laminées. *Rev. Micropaleontol.* **25**, 251-264.
- Krumbein W.E.** (1979). Photolithotrophic and chemoorganotrophic activity of bacteria and algae as related to beach rock formation and degradation (Gulf of Aqaba, Sinai). *Geomicrobiol. J.* **1**, 39-203.
- Lamboy M.** (1990a). Microbial mediation in phosphatogenesis: new data from the Cretaceous phosphatic chalk of northern France. In: *Phosphorite Research and Development* Notholt A.J.G. and I. Jarvis eds. Geol. Soc. London. sp. publ., **52**, 157-167.
- Lamboy M.** (1990b). Microstructure of a phosphatic crust from the Peruvian continental margin: phosphatized bacteria and associated phenomena. *Oceanologica Acta* **13**, 439-451.
- Lamboy M.** (1993) Phosphatization of calcium carbonate in phosphorites: ultrastructure and importance. *Sediment.* **40**, 53-62.
- Lamboy M.** (1994). Nanostructure and genesis of phosphorites from ODP Leg 112, the Peru margin. *Mar. Geol.* **118**, 5-22.
- Lamboy M., Monty C.L.** (1987). Bacterial origin of phosphatized grains. *Terra Cognita* **7**, 207.
- Lamboy, M., Purnachandra Rao V., Ahmed E., Azzouzi N.** (1994). Nanostructure and significance of fish coprolites in phosphorites. *Mar. Geol.* **120**, 373-383.
- Lucas J., Prévôt L.** (1984). Synthèse de l'apatite bactérienne à partir de matière organique phosphatée et de divers carbonates de calcium dans des eaux douce et marine naturelles. *Chem. Geol.* **42**, 101-118.
- Lucas J., Prévôt L.** (1985). The synthesis of apatite by bacterial activity: mechanism. In: *Sciences Géologiques Mem. J.* Lucas and L. Prévôt eds. **77**, 79-81.
- Manheim F., Rowe G.T., Jipa D.** (1975). Marine phosphorite formation off Peru. *J. Sed. Pet.* **45**, 243-251.
- McClellan G.H., Lehr J.R.** (1969). Crystal chemical investigation of natural apatites. *Am. Mineral.* **54**, 1374-1391.

- Monty C.L.** (1976). The origin and development of cryptalgal fabrics. In: *Stromatolites* M.R. Walter ed. Developments in Sedimentology, **20**, Elsevier, 193-249.
- Mountain G.S., Prell W.L.** (1989). Geophysical reconnaissance survey for ODP Leg 117 in the northwest Indian Ocean. In: *Proc. Ocean Drilling Program Initial Reports Leg 117*, Prell W.L. Niitsuma N. et al. eds. College Station, Tx, **117**, 51-64.
- Mullins H.T., Rasch R.F.** (1985). Sea floor phosphorites along the central California continental margin. *Econ. Geol.* **80**, 696-715.
- Murray J., Renard A.F.** (1891). Deep sea deposits. *Rept. Sci. Res. H.M.S. Challenger 1873 - 1876* HMSO London, 525 p.
- O'Brien G.W., Harris J.R., Milnes A.R., Veeh H.H.** (1981). Bacterial origin of East Australian continental margin phosphorites. *Nature* **294**, 442-444.
- O'Brien G.W., Milnes A.R., Veeh H.H., Heggie D.T., Riggs S.R., Cullen D.J., Marshall J.F., Cook P.J.** (1990). Sedimentation dynamics and redox-iron cycling: controlling factors for the apatite-glaucconite association on the East Australian continental margin. In: *Phosphorite Research and Development*. Notholt A.J.G. and I. Jarvis eds. Geol. Soc. London, sp. publ., **52**, 61-86.
- Parker R.J.** (1975). The petrology and origin of some glauconitic and glauco-conglomeratic phosphorites from the South African continental margin. *J. Sediment. Petrol.* **42**, 434-440.
- Parrish J.T.** (1990). Paleooceanographic and paleoclimatic setting of the Miocene phosphogenic episodes. In: *Phosphate deposits of the World - Neogene to Modern phosphorites*, Burnett W.C. and S.R. Riggs eds. Cambridge University Press, **3**, 223-240.
- Pedersen T.F., Shimmield G.B.** (1991). Interstitial water chemistry, Leg 117: contrasts with the Peru margin. In: *Proc. Ocean Drilling Program. Scientific Results Leg 117*, Prell, W.L. Niitsuma, N. et al. eds. College Station, Tx, **117**, 499-551.
- Piper D.Z., Baedeker P.A., Crock J.G., Burnett W.C., Loebner B.J.** (1988). Rare-earth elements in the phosphatic enriched sediment of the Peru shelf. In: *The origin of marine phosphorites: The results of the R.V. Robert, D.Conrad Cruise 23-06 to the Peru shelf*. Burnett W.C. and P.N. Froelich eds. *Mar., Geol.* **80**, 269-285.
- Prell W.L., Niitsuma N. et al.** (1989). *Proc. ODP Initial Reports Leg 117*, College Station, Tx.
- Rao V.P., Burnett W.C.** (1990). Phosphatic rocks and manganese crusts from seamounts in the EEZ of Kiribati and Tuvalu, Central Pacific Ocean. In: *Geology and offshore mineral resources of the Central Pacific Basin*. Keating B.R. and B.R. Bolton eds. Houston, Texas, CircumPacific Council for energy and mineral resources. Earth Science Series, **15**, 285-296.
- Rao V.P., Lamboy M., Natarajen R.** (1992). Possible microbial origin of phosphorites on Error Seamount, Northwestern Arabian Sea. *Mar. Geol.* **106**, 149-164.
- Rao V.P., Nair R.R.** (1988). Microbial origin of the phosphorites of the western continental shelf of India. *Mar. Geol.* **84**, 105-110.
- Rao V.P., Natarajan R., Parthiban G., Mascarenhas A.** (1990). Phosphatised limestones and associated sediments from the western continental shelf of India. *Mar. Geol.* **95**, 17-29.
- Rao V.P., Lamboy M., Dupeuble P.A.** (1993). Verdine and other associated authigenic (glaucony, phosphate) facies from the sediments of the southwestern continental margin of India. *Mar. Geol.* **111**, 133-158.
- Riggs S.R.** (1979). Petrology of the Tertiary phosphorite system of Florida. *Econ. Geol.* **74**, 195-220.
- Soudry D.** (1992). Primary bedded phosphorites in the Campanian Mishash formation, Negev, southern Israel. *Sediment. Geol.* **80**, 77-88.
- Soudry D., Nathan Y.** (1980). Phosphate peloids from the Negev phosphorites. *Jour. Geol. Soc. Lond.* **137**, 749-755.
- Soudry D., Lewy Z.** (1990). Microbially influenced formation of phosphate nodules and megafossil molds (Negev, southern Israel). *Palaeogeogr. Palaeoclimatol. Palaeoecol.* **84**, 15-34.
- Soudry D., Lewy Z.** (1990). Omission surface incipient phosphate crusts on early diagenetic calcareous concretions and their possible origin, Upper Campanian, southern Israel. *Sediment. Geol.* **66**, 151-163.
- Suess E., von Huene R. et al.** (1988). *Proc. ODP Initial Reports 112* College Station, Tx.